Multiwater-Assisted Proton Transfer Study in Glycinamide Using Density Functional Theory

Ping Li[†,‡] and Yuxiang Bu*[,†,‡]

Institute of Theoretical Chemistry, Shandong University, Jinan 250100, P. R. China and Department of Chemistry, Qufu Normal University, Qufu 273165, P. R. China

Received: March 10, 2004; In Final Form: August 28, 2004

Multiwater-assisted proton transfers (PTs) involving two and three water molecules from the amide nitrogen to carbonyl oxygen atom in model peptide compound glycinamide have been investigated employing the B3LYP/6-311++G** level of theory. The thermodynamic and kinetic parameters, such as tautomeric energies, equilibrium constants, barrier heights, and rate constants, have been predicted, respectively. The relevant quantities associated with the proton-transfer processes, such as geometrical structures, interaction energies, and intrinsic reaction coordinate (IRC) calculations, have also been studied. In addition, the factors influencing the thermodynamic and kinetic parameters, such as temperature dependences, solvent effects, and deuteration effects, have also been explored qualitatively, respectively. Computational results show that the PT barrier heights are 16.93 (4.98) and 18.95 (6.67) kcal/mol in the forward (reverse) directions with the assistances of two and three water molecules, which are reduced significantly by 28.43 (25.95) and 26.41 (24.26) kcal/mol compared with those of direct intramolecular PT, respectively. Both of the PT processes proceed with a concerted mechanism, reflecting the bifunctional roles of the water, that is, it can accept a proton from the donor site in glycinamide and transfer a different proton to the acceptor site in glycinamide. The optimal numbers of water molecules directly participating in the PT may be two compared with the barrier heights among the various water-assisted PT cases. Applications of the IPCM model within the framework of the self-consistent reaction filed (SCRF) theory indicate that the bulk solvent has a subtle influence on the thermodynamic and kinetic properties.

1. Introduction

As one of the simplest and the most fundamental phenomena in the tautomeric equilibria and oxidation−reduction reactions, intra- or intermolecular proton transfers (PTs) play an important role in many chemical and biochemical processes.[1,2] A large number of theoretical and experimental studies have been carried out to enrich the information regarding the possible mechanisms of PT, tautomeric equilibria, and relevant properties associated with PT processes.[1−39] In our previous studies,[40] direct and monowater-assisted PTs from the amide nitrogen to the carbonyl oxygen atom in the model peptide compound glycinamide have been investigated at the B3LYP/6-311++G** level of theory. The barrier heights for the direct intramolecular PT are 45.36 and 30.93 kcal/mol for the forward and reverse reactions, respectively, whereas both of them have been reduced significantly by about 26.31 and 24.37 kcal/mol to 19.05 and 6.56 kcal/mol with a single water molecule assisting, which should be easily observable experimentally, especially for the reverse reaction. In particular, the effects of a second water molecule without directly participating in the PT on the tautomeric energies and barrier heights are insignificant. Thus, it is reasonable to further investigate the water-assisted PT in glycinamide excluding the effects of other water molecules without directly participating in the PT.

As one of the important components in glycinamide ribonucleotide synthetase, the relevant investigations of glycinamide have been reported previously theoretically and experimentally.[40−53] For example, the formations of the peptide bond in glycinamide uncatalyzed or catalyzed by the metal cations or ammonia had been extensively studied.[41−44] Klassen et al. reported the collision-induced dissociation threshold energies of protonated glycinamide determined with a modified triple quadrupole mass spectrometer.[45] The unimolecular chemistry of protonated glycinamide and its proton affinity determined by mass spectrometric experiments and theoretical model were reported by Kinser et al.[46] The interrelationship between conformations and theoretical chemical shift was investigated by Sulzbach et al.,[47] in which some useful conformational information was mentioned using the restricted Hartree−Fock (RHF) theory and 6-31G* basis set. Ramek et al. discussed the basis-set influence on the nature of the conformations of glycinamide (minimum or saddle point) in ab initio self-consistent field (SCF) calculations.[48] Recently, multiply sodiated ions were observed by electron-spraying glycinamide and their *N*-acetylated and O-amidated derivatives in the presence of sodium hydroxide, in which some sodiated glycinamide conformers were obtained at the B3LYP/6-311++G** level of theory.[49] The possible conformers of glycinamide in the gas phase and in solution had been systematically explored by us, where three pairs of mirror-image conformers and one *Cs* conformer had been found on the global potential energy surface (PES) of glycinamide at the B3LYP/6-311++G** level of theory.[50,51] More recently, acid−base behaviors for isolated glycinamide had also been investigated,[52] where the calculated proton affinity for the global minimum, 216.81 kcal/mol, is well

* Address correspondence to this author.
† Shandong University.
‡ Qufu Normal University.

10.1021/jp048919i CCC: $27.50
Published on Web 10/23/2004

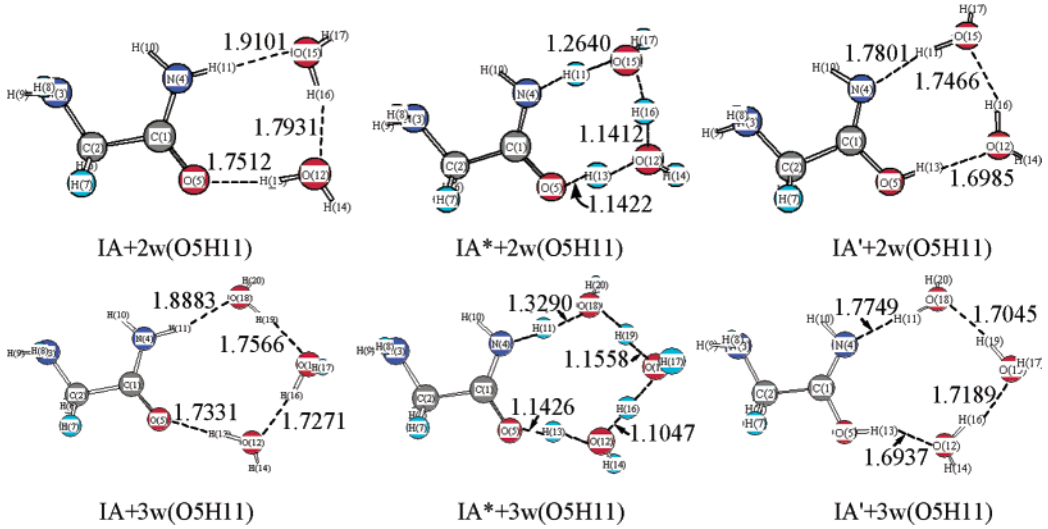

Figure 1. Optimized di- and trihydrated glycinamide complexes and their corresponding tautomeric products along with the transition states connecting them in the gas phase at the B3LYP/6-311++G** level of theory.

consistent with the experimental value 217.23 kcal/mol.[46] Additionally, the ionization potentials and electron affinities of glycinamide in the gas phase and in solution had also been predicted theoretically.[53] In those studies,[50−52] the reliability of the B3LYP/6-311++G** level of theory had been verified through comparisons with higher-level calculations including MP2, MP3, MP4(SDQ), and CCSD(T) levels.

As an expansion of our previous studies,[40] in the present paper, we further investigate the water-assisted PT in glycinamide through inclusions of two and three water molecules without considering the effects of other water molecules not participating in the PT, that is, the PTs are assisted by two and three water molecules by means of the formations of a water-chain bridge connected by the hydrogen of amide and the carbonyl oxygen atoms (see Figure 1). Thus, only the special cyclic hydrated glycinamide complexes have been considered to explore the active roles of the water molecules though many hydrated complexes can be formed through the different interaction modes between glycinamide (or glycinamidic acid) and water molecules, where these active water molecules are located to directly assist the PT. Considering the lack of the experimental data, we expect that the present study can not only fill a void in the available data for glycinamide but also stimulate the experimentalists to further explore the nature of PT mechanisms in larger peptide systems in the future.

2. Computational Details

Using the global minimum **IA** as starting points,[50] we fully optimized the selected di- and trihydrated glycinamide, glycinamidic acid, and their corresponding transition states, where two and three water molecules are specially located to directly participate in the PT since we are most concerned with the role of the water in directly assisting the PT. Normal-mode analyses have been performed to verify that the stable complexes have all positive frequencies and the transition states have only one imaginary frequency with the corresponding eigenvector pointing toward the reactants and products, where none of these frequencies are scaled because of the ability of DFT calculations to predict them accurately as proposed by Johnson.[54] Furthermore, the intrinsic reaction coordinate (IRC)[55,56] calculations in mass-weighted internal coordinates with a step size of 0.1 amu$^{1/2}$ bohr have also been performed to further confirm the validity of the transition states (TSs) connecting the reactants and products.

Consistent with our previous studies,[50−53] the B3LYP/6-311++G** level of theory[57,58] has been employed throughout the calculations since its reliability has been verified previously. Even so, to further validate its reliability in studying the present hydrated complexes, additional calculations, such as the full geometry optimization at the MP2(FULL)/6-311++G** level of theory and single-point energy calculations employing higher levels (MP2(FULL), MP3, MP4(SDQ), and CCSD(T.FULL) levels) and extended basis sets (6-311++G(3df,3pd) and AUG-cc-pVTZ), have also been carried out for those un-, mono-, di-, and trihydrated complexes, where the detailed comparisons among those levels are summarized in the Supporting Information for reference. As mentioned below, all the following discussions are based on the results obtained at the B3LYP/6-311++G** level of theory for the sake of simplicity since its reliability has been verified through comparisons with other levels.

To investigate how the presence of solvent molecules affects the relevant quantities associated with the PT processes mentioned above qualitatively, the isodensity surface-polarized continuum model (IPCM),[59−61] which has been successful in the descriptions of many chemical systems in solution,[53,62−65] has been employed. These calculations are performed on the basis of the optimized gas-phase structures employing a series of solutions, such as chloroform, dichloroethane, acetone, nitromethane, and water (the dielectric constants $\epsilon = 4.9$, 10.36, 20.7, 38.2, and 78.39, respectively).

To evaluate the basis set superposition errors (BSSEs) produced in the calculations of interaction energies between glycinamide or glycinamidic acid and water molecules, the Boys−Bernardi counterpoise technique has been employed.[66]

For the following reaction

$$\text{glycinamide (N4)} \leftrightarrow \text{glycinamidic acid (O5)} \qquad (1)$$

where the direction of the PT from N4 to O5 is defined as the forward reaction and the reverse one is the reaction in the opposite direction. Thus, the equilibrium constant K_p is calculated as

$$K_p = \exp[-\Delta G^\circ/(RT)] \qquad (2)$$

TABLE 1: Selected Geometrical Parameters for Di- and Trihydrated Glycinamide, Glycinamidic Acid Complexes, and Their Corresponding Transition States Connecting Them along with Their Dipole Moments (in Debye) and Rotational Constants (in GHz) Obtained at the B3LYP/6-311++G Level of Theory[a,b]**

para.	IA+2w(O5H11)	IA*+2w (O5H11)	IA′+2w(O5H11)	IA+3w(O5H11)	IA*+3w(O5H11)	IA′+3w(O5H11)
R(1,2)	1.5316	1.5239	1.5219	1.5326	1.5268	1.5236
R(1,4)	1.3380	1.2993	1.2762	1.3359	1.2987	1.2761
R(1,5)	1.2359	1.2874	1.3293	1.2360	1.2823	1.3266
R(2,3)	1.4653	1.4611	1.4601	1.4653	1.4604	1.4602
R(3,8)	1.0139	1.0132	1.0134	1.0138	1.0128	1.0133
R(3,9)	1.0123	1.0115	1.0116	1.0123	1.0113	1.0115
R(4,10)	1.0111	1.0171	1.0213	1.0115	1.0182	1.0223
R(4,11)	1.0226	1.2312	0.9949	1.0238	1.1784	0.9947
A(2,1,4)	115.78	120.45	124.67	115.73	119.45	124.38
A(2,1,5)	118.87	114.07	111.00	118.63	113.60	110.75
A(4,1,5)	125.34	125.48	124.32	125.64	126.95	124.87
A(1,2,3)	113.54	112.64	111.82	113.62	112.83	111.89
A(6,2,7)	106.52	106.25	106.25	106.51	106.24	106.25
A(8,3,9)	107.62	107.99	107.96	107.65	108.13	107.99
A(1,4,10)	116.98	111.93	108.38	116.68	111.46	107.73
D(4,1,2,3)	−12.75	−8.79	−9.15	−12.43	−7.95	−8.98
D(5,1,2,3)	168.25	171.73	171.26	168.54	172.55	171.45
D(2,1,4,10)	0.77	0.42	−0.20	0.59	0.58	0.09
D(2,1,4,11)	−178.50	−179.35	179.66	−177.51	−176.26	−179.18
D(5,1,4,10)	179.70	179.83	179.33	179.54	−179.99	179.59
D(5,1,4,11)	0.43	0.06	0.07	1.44	3.17	1.26
D(1,2,3,8)	−90.81	−95.05	−90.78	−91.00	−97.92	−91.62
D(1,2,3,9)	148.52	143.31	147.86	148.27	139.96	146.91
A[c]	3.799(−2.91)	4.264(3. 80)	3.769(2. 57)	2.295(−3.16)	2.702(-4. 65)	2.404(−2.77)
B	1.020(0. 64)	1.186(0. 10)	1.067(0. 31)	0.669(0.37)	0.776(-0. 45)	0.684(0. 38)
C	0.818(−1.69)	0.942(2. 24)	0.843(1. 99)	0.530(−0.21)	0.613(-0. 57)	0.540(−0.59)
dipole	3.43	4.41	3.27	3.19	4.70	2.85

[a] All the bond lengths (R), bond angles (A), and dihedral angles (D) are in angstroms and degrees, respectively. [b] The data in the rows of R(4,11), D(2,1,4,11), and D(5,1,4,11) refer to those of R(5,13), D(2,1,5,13), and D(4,1,5,13) for the di- and trihydrated glycinamidic acid complexes, respectively. [c] The data in parentheses refer to the dipole moments along the principal axes.

where the $\Delta G°$ refers to the Gibbs free energy change in the PT process. As for the classical forward and reverse rate constants k^{TST}, they can be calculated through the conventional transition-state theory (TST)[3,67,68]

$$k^{TST} = \frac{k_B T}{h} \frac{Q^*}{Q^R} e^{-\Delta E_0^*/(k_B T)} \quad (3)$$

where k_B and h are the Boltzmann and Planck constants; Q^* and Q^R are the equilibrium partition functions for the TS and reactant, and ΔE_0^* is the barrier height corrected with zero-point vibrational energy (ZPVE). Additionally, the quantum mechanical tunneling effect is approximately taken into account through a tunneling transmission coefficient κ with the expression[67,69]

$$\kappa = 1 + \frac{1}{24}\left(\frac{h\upsilon^*}{k_B T}\right)^2 \left(1 + \frac{k_B T}{\Delta E_0^*}\right) \quad (4)$$

where υ^* is the imaginary frequency at the TS. Thus, including the tunneling effect, the final rate constant k is given by

$$k = \kappa k^{TST} \quad (5)$$

All of the computations were performed using the Gaussian 98 program and the SCF convergence criteria *Tight* was used throughout.[70]

3. Results and Discussions

3.1 Structural Features. The optimized di- and trihydrated glycinamide and glycinamidic acid complexes together with their corresponding transition states have been first displayed in Figure 1, where the notations in parentheses stand for the interaction sites of glycinamide with water molecules. Correspondingly, Table 1 lists the selected geometrical parameters together with their rotational constants and dipole moments, where the rotational constants and dipole moments for the dihydrated complexes are larger than those of the trihydrated ones except for the larger dipole moments of the TS in the latter (4.70 versus 4.41 D). Hopefully, the calculated rotational constants and dipole moments should be helpful in the observation or search for these complexes using microwave spectrum and rotational spectroscopy experimentally.

As expected, some geometrical changes take place mainly in the regions of intermolecular H-bonds though the trends are insignificant overall. Similar to those changes of monohydrated glycinamide in which a single water molecule directly participates in the PT,[40] the double-bond and single-bond characters of the peptide bond R(C1−N4) and R(C1−O5) bond (denoted as C1−N4 and C1−O5 for simplicity) in the di- and trihydrated glycinamide complexes have been strengthened, which can be reflected from their different increments in bond lengths of −0.02 and +0.016 Å for the former and the latter with respect to those in the isolated glycinamide, respectively. Furthermore, the lengthening of the N4−H11 (about 0.02 Å) compared with that in isolated glycinamide should be attributed to the formations of the intermolecular H-bond between glycinamide and water, which can be further supported by the red-shift of about 200 cm^{-1} for the stretching vibration between N4 and H11. Actually, as displayed in Figure 1, the shorter distance (1.91 (1.89) Å) between H11 (H11) and O15 (O18) in dihydrated (trihydrated) glycinamide also indicates the existence of the intermolecular H-bond. Similar findings can be also observed between O5 and H13 in the di- and trihydrated glycinamide, where the interatomic distances are 1.75 and 1.73 Å for the former and the latter, respectively. Inspections of the dihedral

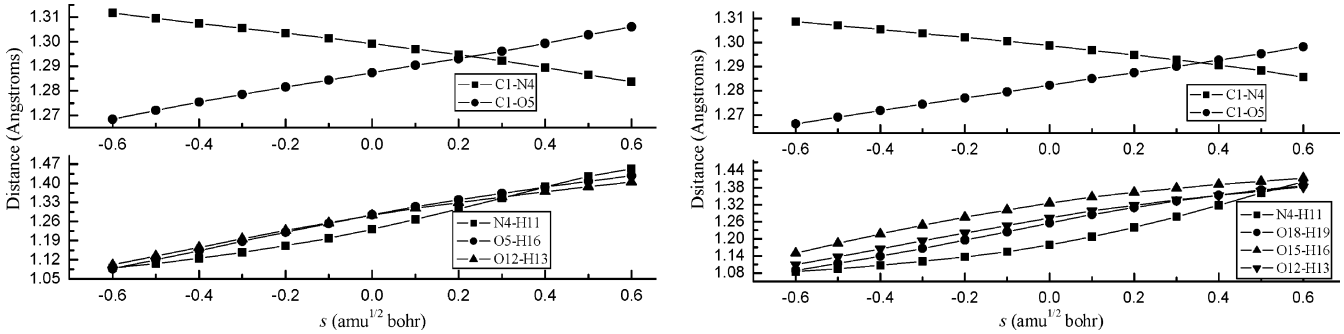

Figure 2. The selected geometrical changes versus reaction coordinate *s* for the IA+2w(O5H11) ↔ IA′+2w(O5H11) (left) and IA+3w(O5H11) ↔ IA′+3w(O5H11) (right) processes.

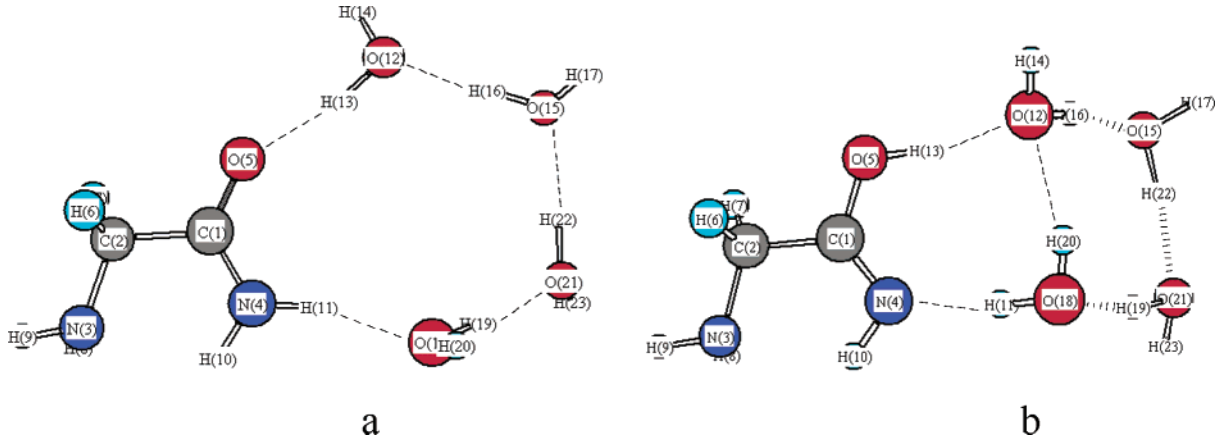

Figure 3. Optimized structures for tetrahydrated glycinamide (a) and glycinamidic acid complexes (b) obtained at the B3LYP/6-311++G** level of theory.

angles suggest that the main skeleton angle D(4,1,2,3) has no significant changes (~1.5°) and the planarity of the peptide bond has still been kept for them.

Like those hydrated glycinamide complexes mentioned above, some structural changes can also be observed for those di- and trihydrated glycinamidic acid complexes compared with the isolated glycinamidic acid.[40] For example, the C1−N4 and C1−O5 bonds have been weakened and strengthened since their increments in bond lengths are about +0.013 and −0.03 Å for the former and the latter, respectively, which is consistent with those occurring in the monowater-assisted case.[40] Compared with isolated glycinamidic acid, both the O5−H13 bonds have been lengthened about 0.03 Å in the di- and trihydrated glycinamidic acid complexes, where the larger elongations of the O5−H13 than those of the N4−H11 bond in hydrated glycinamide complexes mentioned above may imply that the strengths of the intermolecular H-bonds formed between glycinamidic acid and water are larger than those formed between glycinamide and water. Moreover, as displayed in Figure 1, the shorter intermolecular contact distances, such as N4···H11 and O12···H13, relative to those in hydrated glycinamide, such as H11···O15 (or O18) and O5···H13, also indicate the formation of the stronger intermolecular H-bonds in hydrated glycinamidic acid, implying the lowering of the tautomeric energies from glycinamide to glycinamidic acid as described below.

For the transition states, as expected, the bond lengths between heavy atoms, such as C1−N4 and C1−O5, lie in the intermediate between reactants and products in the PT processes, reflecting the transitional nature of them accompanying the PT. Compared with reactants and products, the transition states resemble the products (hydrated glycinamidic acid) more closely than the reactants (hydrated glycinamide). This observation is well consistent with the Hammond's postulates since both tautomeric processes are endothermic reactions from hydrated glycinamide to hydrated glycinamidic acid.[71] Additionally, the key geometrical changes in the PT processes, such as C1−N4 and C1−O5, and especially for those changes of the migrating protons are depicted in Figure 2. Obviously, as described above, the C1−N4 and C1−O5 bonds decrease and increase accompanying the PT, respectively. Especially, inspections of the changes for the migrating protons suggest that the PTs in the di- and trihydrated cases should proceed with a concerted mechanism.

Furthermore, as a tentative study, we have also attempted to explore the PT process assisted directly with four water molecules. As displayed in Figure 3a, the interaction of glycinamide with four water molecules forms a twelve-membered ring structure. According to the main goal of this paper, the proton H11 should be transferred from N4 to O5 along the water-chain bridge formed by four water molecules. However, the optimized tautomeric product, that is, tetrahydrated glycinamidic acid, has a completely different structure as displayed in Figure 3b, where glycinamidic acid interacts with only two water molecules and the other two water molecules interact with the former two water molecules through intermolecular H-bonds, resulting in two eight-membered ring structures. Moreover, the two rings are almost perpendicular to each other (~112°). Obviously, the product does not originate from the reactant by means of PT from the structural point of view. Actually, we have failed to locate the corresponding transition state to the best of our ability. The tetrahydrated glycinamide (Figure 3a) may be a flexible structure with a small frequency (about 17.71 cm^{-1}). Probably, the long-range PT assisted directly with four or even more water molecules is difficult to proceed for glycinamide, where all the water

TABLE 2: The Calculated Interaction Energies $\Delta E_{\text{Interaction}}$ (in kcal/mol), ZPVE, and BSSE Corrections (ΔE_{ZPVE} and ΔE_{BSSE}, in kcal/mol) for the Interactions of Glycinamide and Glycinamidic Acid with Water Molecules[a]

	IA+2w(O5H11)	IA′+2w(O5H11)	IA+3w(O5H11)	IA′+3w(O5H11)
$\Delta E_{\text{Interaction}}$	−20.97(−14.21)	−23.56(−16.40)	−31.29(−20.77)	−33.38(−22.74)
ΔE_{ZPVE}	4.90	5.00	7.41	7.34
ΔE_{BSSE}	1.86	2.16	3.12	3.30

[a] The data in parentheses refer to those corrected with ZPVE and BSSE corrections.

TABLE 3: The Calculated Deformation Energies (in kcal/mol) for Glycinamide, Glycinamidic Acid, and Water Molecules Produced in the Interactions between Them at the B3LYP/6-311++G Level of Theory[a]**

	IA+2w(O5H11)	IA′+2w(O5H11)	IA+3w(O5H11)	IA′+3w(O5H11)
glycinamide	0.66		0.84	
glycinamidic acid		1.73		2.19
1w	0.37	0.71	0.33	0.68
2w	0.25	0.41	0.36	0.45
3w			0.28	0.41

[a] 1w and 2w refer to the $H_{13}O_{12}H_{14}(H_{11}O_{15}H_{17})$ and $H_{16}O_{15}H_{17}$ ($H_{16}O_{12}H_{14}$) moieties in the dihydrated glycinamide (glycinamidic acid) complexes, and 1w, 2w, and 3w refer to the $H_{13}O_{12}H_{14}(H_{11}O_{18}H_{20})$, $H_{16}O_{15}H_{17}(H_{17}O_{15}H_{19})$, and $H_{19}O_{18}H_{20}(H_{14}O_{12}H_{16})$ moieties in the trihydrated glycinamide (glycinamidic acid) complexes, respectively.

TABLE 4: The Calculated Tautomeric Energies ΔE (in kcal/mol), the Changes of Enthalpy ΔH (in kcal/mol), Entropy ΔS (in cal/mol-K), Gibbs Free Energies ΔG (in kcal/mol), and Equilibrium Constants during the PT Processes[a]

processes[b]	ΔE	ΔH	ΔS	ΔG	K_p
IA ↔ IA′[c]	14.32(14.44)	14.31	−0.91	14.59	2.37×10^{-11}
IA+1w(O5H11) ↔ IA′+1w(O5H11)[c]	12.11(12.49)	12.16	−2.87	13.02	3.26×10^{-10}
IA+2w(O5H11) ↔ IA′+2w(O5H11)	11.73(11.95)	11.60	−3.31	12.58	6.82×10^{-10}
IA+3w(O5H11) ↔ IA′+3w(O5H11)	12.22(12.28)	11.99	−2.35	12.69	5.65×10^{-10}

[a] The data in parentheses refer to those corrected with ZPVEs. [b] These processes are written as 0, 1, 2, and 3 from top to bottom in Table 5 for simplicity, respectively. [c] The data in ref 40.

molecules directly participate in the PT process. Of course, more sophisticated investigations are required to further verify this point soon.

3.2 Interaction Energies. Table 2 summarizes the calculated interaction energies between glycinamide, glycinamidic acid, and water molecules, where the interaction energy is defined as the energy difference between the optimized hydrated complexes and the sums of the optimized monomers including the ZPVE and BSSE corrections.

As displayed in Figure 1, all the di- and trihydrated complexes are stabilized by the formations of intermolecular H-bonds, where all of them possess cyclic 8- and 10-membered ring structures for the former and the latter, respectively. For the interaction of glycinamide with two water molecules, its interaction energy is smaller than that of corresponding glycinamidic acid, where the interaction energies are −20.97 (−14.21) and −23.56 (−16.40) kcal/mol without (with) ZPVE and BSSE corrections for the former and the latter, respectively. Furthermore, the interaction energies become larger with additional stabilization of 6.56 (6.34) kcal/mol for trihydrated glycinamide (glycinamidic acid) considering ZPVE and BSSE corrections. These above phenomena may be rationalized by the existence of the stronger intermolecular H-bond in hydrated glycinamidic acid complexes as mentioned above. Obviously, further inclusions of ZPVE and BSSE corrections lower the interaction energies by about 7.0 and 10.6 kcal/mol for the di- and trihydrated cases, suggesting the importance of them in calculating the interactions between molecules, where the contributions of ZPVE corrections to overall interaction energies are larger (ranging from 30.5 to 35.7%) than those of BSSE corrections (ranging from 13.1 to 15.0%). Additionally, as expected, the values of ZPVE and BSSE corrections produced in trihydrated cases are larger than those of values in dihydrated ones as listed in Table 2.

Table 3 presents the calculated deformation energies for the species participating in the PT, where the deformation energy is defined as the energy difference between the neutral states at the geometries in the hydrated complexes and those in their corresponding optimized isolated states qualitatively. Consistent with our previous findings,[40] the deformation energies of glycinamide upon di- and trihydration are smaller than those of corresponding glycinamidic acid, suggesting the ability of glycinamidic acid to form stronger intermolecular H-bonds with water molecules in the selected hydrated complexes in which the water molecules directly participate in the PT. Similarly, the larger deformation energies of water molecules in hydrated glycinamidic acid complexes relative to those in hydrated glycinamide complexes also support this point.

3.3 Thermodynamic and Kinetic parameters. *3.3.1 Thermodynamics.* Table 4 summarizes the calculated tautomeric energies, equilibrium constants, ΔH, ΔS, and ΔG in the tautomeric processes together with corresponding results of the direct and monowater-assisted PT for comparison.

For both water-assisted tautomeric processes, that is, **IA+2w(O5H11) → IA′+2w(O5H11)** and **IA+3w(O5H11) → IA′+3w(O5H11)**, the tautomeric energies are 11.73 (11.95) and 12.22 (12.28) kcal/mol without (with) ZPVE corrections, indicating that glycinamide is more stable than glycinamidic acid. This point can be further reflected from the calculated potential energy curves versus reaction coordinates as depicted in Figure 4 qualitatively. Comparisons of the tautomeric energies before and after ZPVE corrections indicate that the ZPVE corrections have a subtle influence on the calculated tautomeric energies though inclusions of them slightly disfavor the tautomeric processes. Compared with that of direct tautomeric process, as listed in Table 4, the participations of water molecules lower the tautomeric energy more or less, where the dihydrated case possesses the smallest tautomeric energy. As described above,

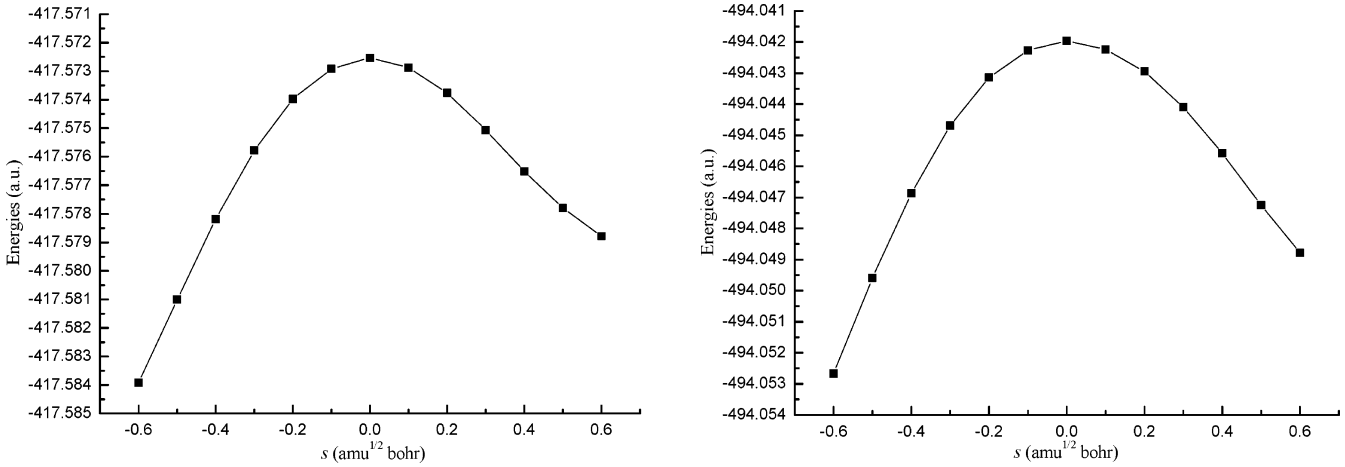

Figure 4. The calculated potential energy curves versus reaction coordinate *s* for the IA+2w(O5H11) ↔ IA′+2w(O5H11) (left) and IA+3w(O5H11) ↔ IA′+3w(O5H11) (right) processes.

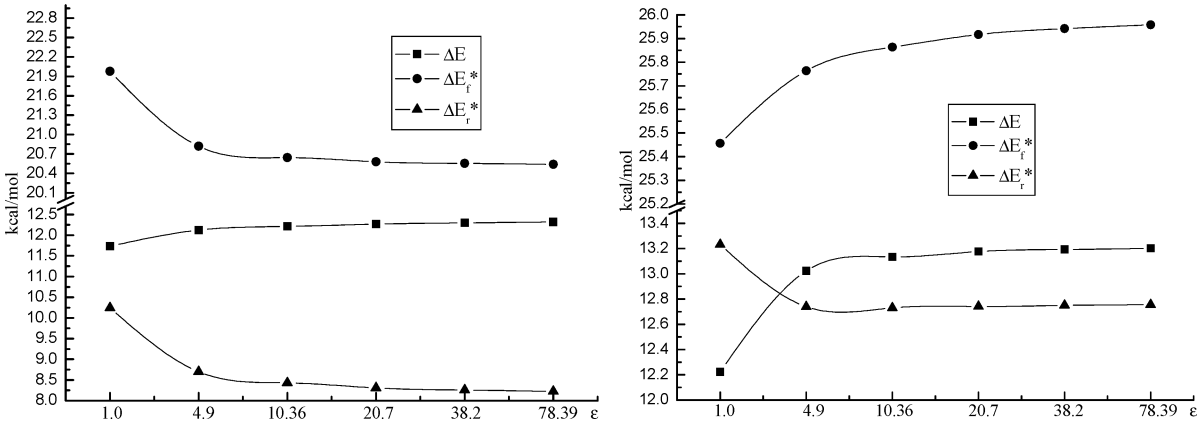

Figure 5. The dependences of forward, reverse barrier heights, and tautomeric energy changes on various dielectric constants for the IA+2w(O5H11) ↔ IA′+2w(O5H11) (left) and IA+3w(O5H11) ↔ IA′+3w(O5H11) (right) processes.

this point can be elucidated from the stronger intermolecular H-bonds formed in hydrated glycinamidic acid relative to those in corresponding hydrated glycinamide. Additionally, the dependences of the tautomeric energies on the dielectric constants have been illustrated in Figure 5 on the basis of the IPCM model within the framework of the SCRF theory. Obviously, the presence of bulk solvent increases the tautomeric energies slightly relative to those in the gas phase though the increments are relatively small with the increasing of dielectric constants. These changing trends can be understood since the solvation energies are slightly favorable for hydrated glycinamide complexes over those of corresponding hydrated glycinamidic acid forms, which is also consistent with their relative orders in dipole moments as listed in Table 1.

As also shown in Table 4, all the positive values of ΔH, ranging from 11.6 to 14.31 kcal/mol, indicate that all the tautomeric processes should be endothermic reactions. The relatively small values for ΔS show that the ΔG should be essentially governed by ΔH in the tautomeric processes. Additionally, the dependences of ΔH, ΔS, and ΔG on temperature have been illustrated in Figure 6. Obviously, both tautomeric processes assume the similar changing trends for them with the increasing of temperature. From the viewpoint of thermodynamics, the water-assisted tautomeric processes should be favorable to proceed at low temperature because the ΔG increases with the increasing of temperature. Overall, the changes of these thermodynamic parameters caused by the direct introductions of two and three water molecules are relatively small.

Figure 7 displays the temperature dependences of equilibrium constants K_p for both water-assisted tautomeric processes. Obviously, both of them assume almost the similar trends, that is, they increase with the increasing of temperature. In general, the increasing of the temperature should be in favor of the proceeding of the reaction kinetically. On the other hand, as mentioned above, the water-assisted tautomeric processes should be favorable to proceed at low temperature thermodynamically. As a result, the interplay of both factors cause the present changing trends. Thus, comparing the calculated tautomeric energies, Gibbs free energy changes, and equilibrium constants among the various water-assisted cases studied here, we can draw a preliminary conclusion that the direct participation of two water molecules may be most favorable in catalyzing the tautomeric processes thermodynamically, where the results at the MP2(FULL) full optimization level also support this point as illustrated in Table S4 of the Supporting Information.

3.3.2 Kinetics. Table 5 summarizes the relevant kinetic parameters, such as barrier heights, rate constants, and tunneling coefficients calculated at 300 K and 1.0 atm.

For the PT processes assisted with two and three water molecules, their corresponding barrier heights are 16.93 (4.98) and 18.95 (6.67) kcal/mol with ZPVE corrections for the forward (reverse) reactions, which are significantly smaller than those of the direct intramolecular PT as shown in Table 5. Thus, the lower barrier heights in the water-assisted PT processes indicate that the direct participations of water molecules should enable the kinetically difficult PT process to take place more easily. Compared with the PT assisted with a single water molecule,[40]

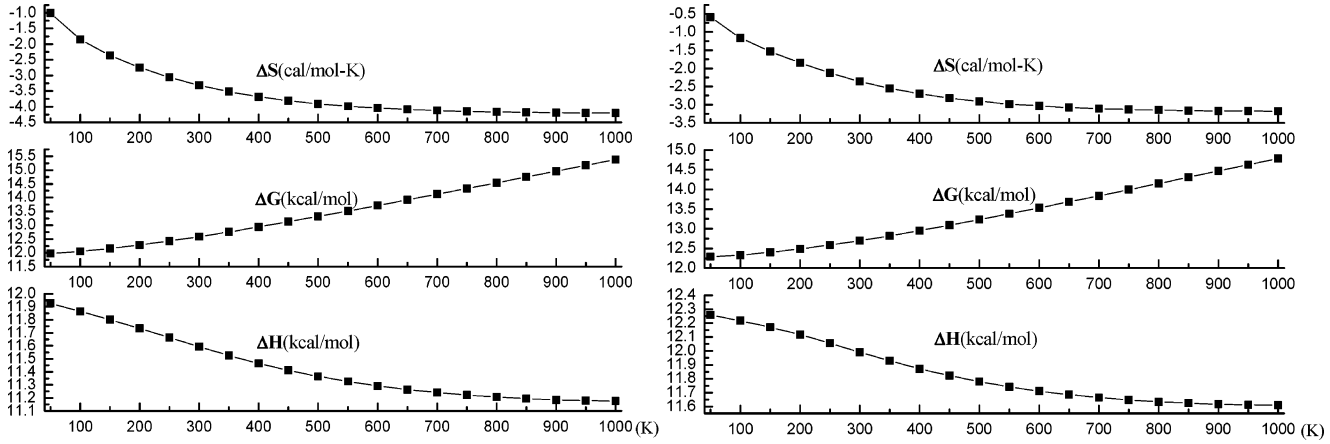

Figure 6. The dependences of the changes of enthalpy, entropy, and Gibbs free energy on various temperatures for the IA+2w(O5H11) → IA′+2w-(O5H11) (left) and IA+3w(O5H11) → IA′+3w(O5H11) (right) processes.

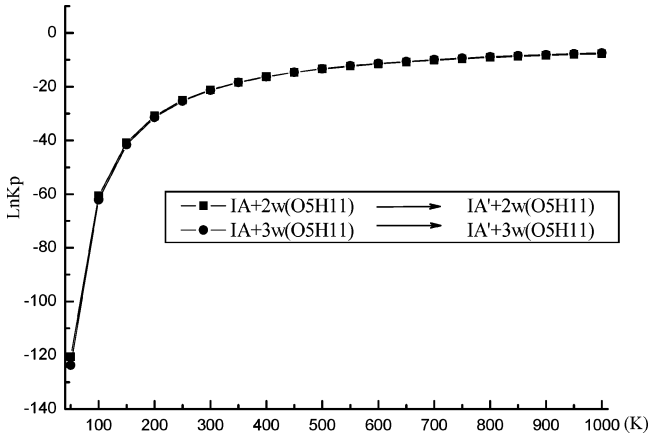

Figure 7. The dependences of the natural logarithms of equilibrium constants on various temperatures for the IA+2w(O5H11) → IA′+2w-(O5H11) and IA+3w(O5H11) → IA′+3w(O5H11) processes.

the barrier heights have been reduced by about 2.12 (1.21) and 1.58 (0.84) kcal/mol for the forward and reverse reactions with the assistance of two water molecules, where the data in parentheses refer to those of the MP2(FULL) full optimization level. Further introductions of a third water molecule increase the barrier heights by additional 2.02 (2.49) and 1.69 (2.18) kcal/mol for the forward and reverse reactions compared with those of dihydrated case at B3LYP (MP2(FULL)) optimization level. Thus, the optimal number of water molecule should be two if only the barrier heights are considered among the three water-assisted PT processes kinetically, which is also reproduced by the comparisons among the calculated barrier heights at the MP2(FULL) full optimization level as illustrated in Table S4 of the Supporting Information. Additionally, as displayed in Table 5, inclusions of ZPVE corrections lower the barrier heights in both directions in all cases, especially in those water-assisted PT processes. What is more, the degree of reduction increases with the increasing of the number of water molecules, where the barrier heights in the forward (reverse) directions have been reduced by about 3.40 (3.51), 3.51 (3.89), 5.05 (5.27), and 6.51 (6.56) kcal/mol for the un-, mono-, di-, and trihydrated systems, respectively. Analogous to the findings of Zhang et al.,[16] this phenomenon can be elucidated from the primary source of the ZPVE corrections qualitatively, that is, the difference in the ground-state energies of the active bonds in the reactant and transition state. For example, for the forward reaction in the isolated glycinamide, there is only one N−H active bond. However, in the mono-, di-, and trihydrated glycinamide complexes, one, two, and three additional O−H active bonds are involved in the reactions. The ZPVE corrections should be negative since all these active bonds are stretched at the transition states. Naturally, the larger ZPVE corrections can be obtained when more active bonds are involved.[16]

In particular, as an important finding, the barrier heights in both directions are correlated with the extent to which the angle A(O5C1N4) is bent. In other words, the larger the degree of expansion (or compression) of A(O5C1N4) is, the higher the barrier height is. For example, the A(O5C1N4) is changed by −16.57° (−13.28°), −3.48° (−1.65°), 0.14° (1.15°), and 1.32° (2.08°) for the transition state with respect to reactant (product) in un-, mono-, di-, and trihydrated cases, respectively, where the positive and negative symbols suggest that the angle A(O5C1N4) becomes expansion and compression in TS. At the same time, the barrier heights are 45.36 (30.93), 19.05 (6.56), 16.93 (4.98), and 18.95 (6.67) kcal/mol in these corresponding processes, respectively. Thus, the catalytic role of water molecules should be completed through the lowering of the degrees of the changing of A(O5C1N4). This phenomenon

TABLE 5: The Calculated Barrier Heights ΔE^* (in kcal/mol), Rate Constants Corrected with and without Considering Tunneling Coefficients (in s^{-1}), and Tunneling Coefficients for the Forward and Reverse Reactions (Noted with Footnotes f and r, Respectively) in the PT Processes[a]

processes[b]	ΔE_f^*	k_f^{TST}	k_f	κ_f	ΔE_r^*	k_r^{TST}	k_r	κ_r
0	48.76(45.36)	4.51×10^{-21}	2.08×10^{-20}	4.61	34.44(30.93)	1.91×10^{-10}	8.75×10^{-10}	4.58
1	22.56(19.05)	7.92×10^{-3}	2.49×10^{-2}	3.14	10.45(6.56)	2.43×10^{7}	7.31×10^{7}	3.01
2	21.98(16.93)	1.31×10^{-1}	3.50×10^{-1}	2.70	10.25(4.98)	1.93×10^{8}	4.89×10^{8}	2.53
	(17.93)[c]	*1.56×10^{-2}*	*3.41×10^{-2}*	*2.18*	*(6.07)*	*2.24×10^{7}*	*4.71×10^{7}*	*2.10*
3	25.46(18.95)	2.52×10^{-3}	5.85×10^{-3}	2.32	13.23(6.67)	4.49×10^{6}	1.01×10^{7}	2.24
	(20.54)[c]	*1.14×10^{-4}*	*2.11×10^{-4}*	*1.85*	*(8.31)*	*2.13×10^{5}*	*3.85×10^{5}*	*1.81*

[a] The data in parentheses refer to those corrected with ZPVEs. [b] See the notation b of Table 4. [c] The italics refer to the corresponding results including the deuteration effects.

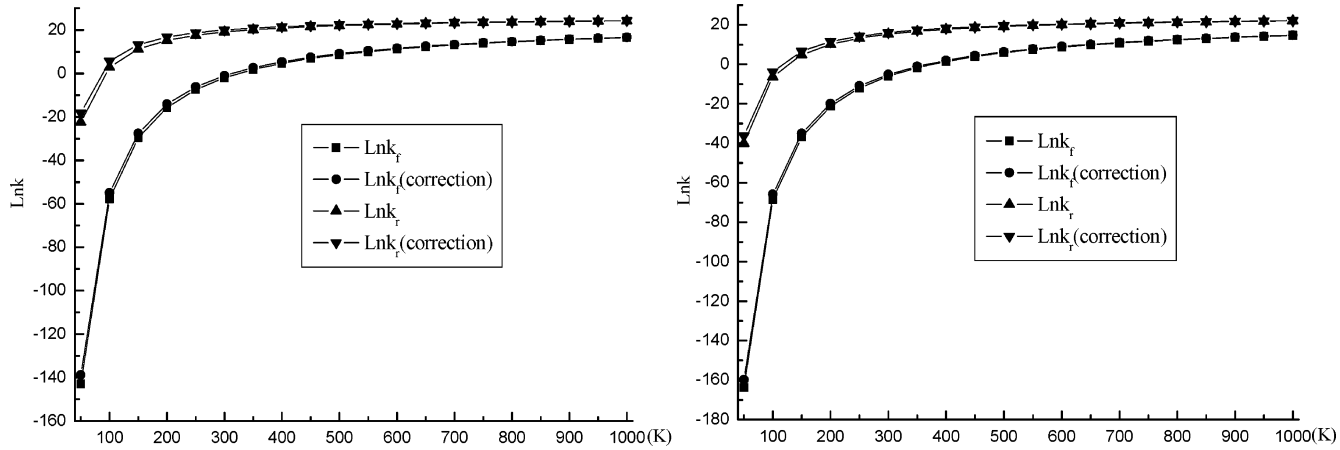

Figure 8. The dependences of the natural logarithms of rate constants on various temperatures for the IA+2w(O5H11) ↔ IA′+2w(O5H11) (left) and IA+3w(O5H11) ↔ IA′+3w(O5H11) (right) processes.

should be a good example in the PT processes occurring in the most biological systems.

As displayed in Figure 5, the solvent effects on the barrier heights have been evaluated qualitatively employing the IPCM model on the basis of the optimized gas-phase geometries. Consistent with our previous studies,[40] the existences of bulk solvent have only slight influences on the barrier heights overall compared with the reductions of the barrier height in the water-assisted PT processes versus those of the direct intramolecular PT process, where the largest changes in solution are about 1.44 and 2.03 kcal/mol for the forward and reverse directions compared with those without considering solvent effects. As expected, the barrier heights decrease with the increasing of dielectric constants in the dihydrated case, which is well correlated with the fact that the transition state has a larger dipole moment relative to its reactant and product. Unexpectedly, the changing trend, that is, the forward barrier height gradually increases in the trihydrated case, cannot be elucidated only from the size of the dipole moments though the changes are very small. Probably, other factors, such as local dipoles and higher multipole moments, should play an important role for the solvent stabilization of the trihydrated glycinamide. Considering the fact that the IPCM model adopted here cannot represent the realistic situation in the biological medium for these hydrated complexes, we expect that more accurate predictions for the solvent effects on the PT processes kinetically should be required in the future with more accurate solvation models.

As listed in Table 5, the water-assisted PT rate constants are much larger than those of the direct intramolecular PT. Further inclusions of the quantum mechanical tunneling effects increase the PT rate constants, where the values of the tunneling coefficients, ranging from 2.32 to 2.70 and from 2.24 to 2.53 for the forward and reverse reactions at room temperature, suggest that it is important to consider the quantum mechanical effects in the present study.

Additionally, the temperature dependences of the rate constants corrected with and without considering tunneling coefficients have been illustrated in Figure 8. Obviously, all of them increase dramatically before around 300 K and then increase gradually with the increasing of temperature. As expected, the tunneling effects decrease gradually with the increasing of temperature and become less important when temperature exceeds 500 K.

Tentatively, the deuteration effects have also been explored qualitatively, that is, the hydrogen atoms in water molecules have been substituted by deuterium atoms. Some findings can be observed as follows compared with those without deuterated cases. First, the deuteration effects on the vibrational modes at the transition states are not remarkable, where all of them still remain almost the same as those without deuterated cases. On the other hand, the unique imaginary frequency in the di- and trihydrated cases has been reduced from 1347.2 and 1194.2 cm^{-1} to 1128.5 and 953.2 cm^{-1}, respectively, exhibiting the deuteration effects apparently. Second, the barrier heights increase by about 1.0 (1.09) and 1.59 (1.64) kcal/mol for the forward (reverse) reactions in the deuterated di- and trihydrated cases. Correspondingly, the calculated rate constants also decrease as displayed in Table 5. Finally, as expected, the calculated tunneling coefficients are smaller than those corresponding values before deuteration. All these above findings are predicted qualitatively on the basis of the conventional transition-state theory plus tunneling corrections. Further study is expected to better understand the deuteration effects with more sophisticated kinetic models.

In conclusion, comparisons of the barrier heights and rate constants indicate that the water molecules should play a key role in assisting the PT. Especially for the dihydrated case, it has the smallest barrier heights in both directions and the largest rate constants compared with those of the mono- and trihydrated cases. Probably, the water-assisted PT should proceed preferentially with the assistance of two water molecules statically. On the other hand, the probability of the other water-assisted PTs, such as mono- and trihydrated cases, should not be ruled out since they have slightly higher barrier heights compared with dihydrated case before the nature of the water-assisted PTs in glycinamide has been confirmed experimentally. Moreover, the predicted feasibility of the PT theoretically should be helpful to the experimentalists specialized in this area.

4. Conclusions

In the present study, the multiwater-assisted PTs in glycinamide involving two and three water molecules have been investigated employing the B3LYP/6-311++G** level of theory. The relevant geometries and the interactions produced in the PT processes have been discussed, respectively. More importantly, the thermodynamic and kinetic properties especially, such as tautomeric energies, equilibrium constants, barrier heights, and rate constants, have also been predicted. Additionally, the temperature dependences, solvent effects, and deuteration effects on those thermodynamic and kinetic parameters have been explored, respectively. The principal conclusions from this study are as follows:

1. In the water-assisted tautomeric processes, the strengths of the intermolecular H-bond formed between glycinamidic acid and water are larger than those formed between glycinamide and water, resulting in the reductions of the tautomeric energy compared with that of direct intramolecular PT in isolated glycinamide.

2. In the water-assisted PT processes, the migrating protons are transferred with a concerted mechanism along a water-chain bridge formed by the water molecules. The corresponding barrier heights are correlated with the extent to which the angle A(O5C1N4) is bent, that is, the larger the degree of the expansion (or compression) of the A(O5C1N4) is, the higher the barrier height is.

3. Compared with that of the direct intramolecular PT, the direct participations of the water molecules reduce the barrier heights significantly by about 26.31 (24.37), 28.43 (25.95), and 26.41 (24.26) kcal/mol to 19.05 (6.56), 16.93 (4.98), and 18.95 (6.67) kcal/mol for the forward (reverse) reactions in the mono-, di-, and trihydrated cases, implying that the water-assisted PT processes should be easily observable at any temperature of biological importance if possible experimentally. Obviously, the dihydrated case provides an optimal static condition among the various water-assisted cases studied here.

4. The existence of the bulk solvent has a subtle influence on the thermodynamic and kinetic parameters.

Acknowledgment. This work is supported by the National Natural Science Foundation of China (20273040) and the Natural Science Foundation of Shandong Province (Key project), and the support from SRFDP and the Foundation for University Key Teacher by the Ministry of Education of China is also acknowledged. We are also grateful to the referees for their insightful suggestions to improve the presentation of the results.

Supporting Information Available: Figure S1 displays the studied complexes for the un-, mono-, di-, and trihydrated glycinamide complexes and their corresponding tautomeric products along with the transition states connecting them. Correspondingly, the standard orientations for those complexes at both the B3LYP/6-311++G** and MP2(FULL)/6-311++G** levels of theory have been summarized in Table S1. Table S2 presents the selected single-point energy calculations for the studied complexes in Figure S1 at the B3LYP/6-311++G** and MP2(FULL)/6-311++G** levels of theory. The calculated interaction energies, ZPVE corrections, and BSSE corrections for the interactions of glycinamide and glycinamidic acid with water molecules at the B3LYP/6-311++G** and MP2(FULL)/6-311++G** levels of theory have been summarized in Table S3. Finally, Table S4 presents the calculated tautomeric energies and barrier heights for the studied tautomeric processes at various levels of theory. This material is available free of charge via the Internet at http://pubs.acs.org.

References and Notes

(1) Desiraju, G. R. *Acc. Chem. Res.* **1991**, *24*, 290.
(2) Hibbert, F. *Adv. Phys. Org. Chem.* **1986**, *22*, 113.
(3) Zhang, K.; Chung-Phillips, A. *J. Chem. Inf. Comput. Sci.* **1999**, *39*, 382.
(4) Gorb, L.; Leszczynski, J. *Int. J. Quantum Chem.* **1998**, *70*, 855.
(5) Venkateswarlu, D.; Leszczynski, J. *J. Phys. Chem. A* **1998**, *102*, 6161.
(6) Gorb, L.; Leszczynski, J. *J. Am. Chem. Soc.* **1998**, *120*, 5024.
(7) Gu, J.; Leszczynski, J. *J. Phys. Chem. A* **1999**, *103*, 577.
(8) Gu, J.; Leszczynski, J. *J. Phys. Chem. A* **1999**, *103*, 2744.
(9) Zhanpeisov, N. U.; Cox, W. W., Jr; Leszczynski, J. *J. Phys. Chem. A* **1999**, *103*, 4564.
(10) Shukla, M. K.; Leszczynski, J. *J. Phys. Chem. A* **2000**, *104*, 3021.
(11) Podolyan, Y.; Gorb, L.; Leszczynski, J. *J. Phys. Chem. A* **2002**, *106*, 12103.
(12) Gorb, L.; Podolyan, Y.; Leszczynski, J.; Siebrand, W.; Fernández-Ramos, A.; Smedarchina, Z. *Biopolymers* **2002**, *61*, 77.
(13) Wang, X.; Nichols, J.; Feyereisen, M.; Gutowski, M.; Boatz, J.; Haymet, A. D. J.; Simons, J. *J. Phys. Chem.* **1991**, *95*, 10419.
(14) Bell, R. L.; Taveras, D. L.; Truong, T. N.; Simons, J. *Int. J. Quantum Chem.* **1997**, *63*, 861.
(15) Bell, R. L.; Truong, T. N. *J. Chem. Phys.* **1994**, *101*, 10442.
(16) Zhang, Q.; Bell, R.; Truong, T. N. *J. Phys. Chem.* **1995**, *99*, 592.
(17) (a) Scheiner, S.; Kern, C. W. *J. Am. Chem. Soc.* **1979**, *101*, 4081. (b) Scheiner, S.; Wang, L. *J. Am. Chem. Soc.* **1993**, *115*, 1958.
(18) (a) Bertran, J.; Oliva, A.; Rodríguez-Santiago, L.; Sodupe, M. *J. Am. Chem. Soc.* **1998**, *120*, 8159. (b) Rodríguez-Santiago, L.; Sodupe, M.; Oliva, A.; Bertran, J. *J. Am. Chem. Soc.* **1999**, *121*, 8882.
(19) Pranata, J.; Davis, G. D. *J. Phys. Chem.* **1995**, *99*, 14340.
(20) (a) Nguyen, K. A.; Gordon, M. S.; Truhlar, D. G. *J. Am. Chem. Soc.* **1991**, *113*, 1596. (b) Gordon, M. S. *J. Phys. Chem.* **1996**, *100*, 3974. (c) Chaban, G. M.; Gordon, M. S. *J. Phys. Chem. A* **1999**, *103*, 185.
(21) Wu, D. H.; Ho, J. J. *J. Phys. Chem. A* **1998**, *102*, 3582.
(22) Yen, S. J.; Lin, C. Y.; Ho, J. J. *J. Phys. Chem. A* **2000**, *104*, 11771.
(23) Rodriquez, C. F.; Cunje, A.; Shoeib, T.; Chu, I. K.; Hopkinson, A. C.; Siu, K. W. M. *J. Phys. Chem. A* **2000**, *104*, 5023.
(24) Lim, J.-H.; Lee, E. K.; Kim, Y. *J. Phys. Chem. A* **1997**, *101*, 2233.
(25) Kim, Y. *J. Am. Chem. Soc.* **1996**, *118*, 1522.
(26) Kim, Y.; Lim, S.; Kim, H.-J.; Kim, Y. *J. Phys. Chem. A* **1999**, *103*, 617.
(27) Kim, Y.; Lim, S.; Kim, Y. *J. Phys. Chem. A* **1999**, *103*, 6632.
(28) Florián, J.; Hrouda, V.; Hobza, P. *J. Am. Chem. Soc.* **1994**, *116*, 1457.
(29) Florián, J.; Leszczyński, J. *J. Am. Chem. Soc.* **1996**, *118*, 3010.
(30) Minyaev, R. M. *Chem. Phys. Lett.* **1996**, *262*, 194.
(31) Adamo, C.; Cossi, M.; Barone, V. *J. Comput. Chem.* **1997**, *18*, 1993.
(32) Pan, Y.; McAllister, M. A. *J. Am. Chem. Soc.* **1997**, *119*, 7561.
(33) Lu, D.; Voth, G. A. *J. Am. Chem. Soc.* **1998**, *120*, 4006.
(34) Kryachko, E. S.; Nguyen, M. T. *J. Phys. Chem. A* **2001**, *105*, 153.
(35) Chaudhuri, C.; Jiang, J. C.; Wu, C.-C.; Wang, X.; Chang, H.-C. *J. Phys. Chem. A* **2001**, *105*, 8906.
(36) Taylor, J.; Eliezer, I.; Sevilla, M. D. *J. Phys. Chem. B* **2001**, *105*, 1614.
(37) Tatara, W.; Wójcik, M. J.; Lindgren, J.; Probst, M. *J. Phys. Chem. A* **2003**, *107*, 7827.
(38) Cui, Q.; Karplus, M. *J. Phys. Chem. B* **2003**, *107*, 1071.
(39) Kulhánek, P.; Schlag, E. W.; Koča, J. *J. Am. Chem. Soc.* **2003**, *125*, 13678.
(40) Li, P.; Bu, Y. *J. Phys. Chem. B*, in revision.
(41) Oie, T.; Loew, G. H.; Burt, S. K.; MacElroy, R. D. *J. Am. Chem. Soc.* **1984**, *106*, 8007.
(42) (a) Jensen, J. H.; Baldridge, K. K.; Gordon, M. S. *J. Phys. Chem.* **1992**, *96*, 8340. (b) Jensen, J. H.; Gordon, M. S. *J. Am. Chem. Soc.* **1995**, *117*, 8159.
(43) Remko, M.; Rode, B. M. *Chem. Phys. Lett.* **2000**, *316*, 489.
(44) Remko, M.; Rode, B. M. *Phys. Chem. Chem. Phys.* **2001**, *3*, 4667.
(45) Klassen, J. S.; Kebarle, P. *J. Am. Chem. Soc.* **1997**, *119*, 6552.
(46) Kinser, R. D.; Ridge, D. P.; Hvistendahl, G.; Rasmussen, B.; Uggerud, E. *Chem.−Eur. J.* **1996**, *2*, 1143.
(47) Sulzbach, H. M.; Schleyer, P. V. R.; Schaefer, H. F., III. *J. Am. Chem. Soc.* **1994**, *116*, 3967.
(48) Ramek, M.; Cheng, V. K. W. *Int. J. Quantum Chem., Quantum Boil. Symp.* **1992**, *19*, 15.
(49) Grewal, R. N.; Aribi, H. E.; Smith, J. C.; Rodriquez, C. F.; Hopkinson, A. C.; Siu, K. W. M. *Int. J. Mass Spectrom.* **2002**, *219*, 89.
(50) Li, P.; Bu, Y.; Ai, H. *J. Phys. Chem. A* **2003**, *107*, 6419.
(51) Li, P.; Bu, Y.; Ai, H. *J. Phys. Chem. B* **2004**, *108*, 1405.
(52) Li, P.; Bu, Y.; Ai, H. *J. Phys. Chem. A* **2004**, *108*, 4069.
(53) Li, P.; Bu, Y.; Ai, H. *J. Phys. Chem. A* **2004**, *108*, 1200.
(54) Johnson, B. G.; Gill, P. M. W.; Pople, J. A. *J. Chem. Phys.* **1993**, *98*, 5612.
(55) Gonzalez, C.; Schlegel, H. B. *J. Chem. Phys.* **1989**, *90*, 2154.
(56) Gonzalez, C.; Schlegel, H. B. *J. Phys. Chem.* **1990**, *94*, 5523.
(57) Becke, A. D. *J. Chem. Phys.* **1993**, *98*, 5648.
(58) Lee, C.; Yang, W.; Parr, R. G. *Phys. Rev. B* **1988**, *37*, 785.
(59) Barone, V.; Cossi, M.; Tomasi, J. *J. Comput. Chem.* **1998**, *19*, 404.
(60) Barone, V.; Cossi, M. *J. Phys. Chem. A* **1998**, *102*, 1995.
(61) Foresman, J. B.; Keith, T. A.; Wiberg, K. B.; Snoonian, J.; Frisch, M. J. *J. Phys. Chem.* **1996**, *100*, 16098.
(62) Li, X.; Sevilla, M. D.; Sanche, L. *J. Am. Chem. Soc.* **2003**, *125*, 8916.
(63) Li, X.; Sanche, L.; Sevilla, M. D. *J. Phys. Chem. A* **2002**, *106*, 11248.
(64) Lee, I.; Kim, C. K.; Han, I. S.; Lee, H. W.; Kim, W. K.; Kim, Y. B. *J. Phys. Chem. B* **1999**, *103*, 7302.

(65) Kovacevic, B.; Maksic, Z. B. *Org. Lett.* **2001**, *3*, 1523.
(66) Boys, S. F.; Bernardi, F. *Mol. Phys.* **1970**, *19*, 553.
(67) Jensen, J. H.; Gordon, M. S. *J. Am. Chem. Soc.* **1991**, *113*, 7917.
(68) Steinfiled, J. I.; Francisco, J. S.; Hase, W. L. *Chemical Kinetic and Dynamics*; Prentice Hall: Englewood Cliffs, NJ, 1989.
(69) Wigner, E. *Z. Phys. Chem. B* **1932**, *19*, 203.
(70) Frisch, M. J.; Trucks, G. W.; Schlegel, H. B.; Scuseria, G. E.; Robb, M. A.; Cheeseman, J. R.; Zakrzewski, V. G.; Montgomery, J. A., Jr.; Stratmann, R. E.; Burant, J. C.; Dapprich, S.; Millam, J. M.; Daniels, A. D.; Kudin, K. N.; Strain, M. C.; Farkas, O.; Tomasi, J.; Barone, V.; Cossi, M.; Cammi, R.; Mennucci, B.; Pomelli, C.; Adamo, C.; Clifford, S.; Ochterski, J.; Petersson, G. A.; Ayala, P. Y.; Cui, Q.; Morokuma, K.; Malick, D. K.; Rabuck, A. D.; Raghavachari, K.; Foresman, J. B.; Cioslowski, J.; Ortiz, J. V.; Stefanov, B. B.; Liu, G.; Liashenko, A.; Piskorz, P.; Komaromi, I.; Gomperts, R.; Martin, R. L.; Fox, D. J.; Keith, T.; Al-Laham, M. A.; Peng, C. Y.; Nanayakkara, A.; Gonzalez, C.; Challacombe, M.; Gill, P. M. W.; Johnson, B.; Chen, W.; Wong, M. W.; Andres, J. L.; Gonzalez, C.; Head-Gordon, M.; Replogle, E. S.; Pople, J. A. Gaussian, Inc.: Pittsburgh, PA, 1998.
(71) Hammond, G. S. *J. Am. Chem. Soc.* **1955**, *77*, 334.